Vascular targeted single-walled carbon nanotubes for near-infrared light therapy of cancer

Vascular targeted single-walled carbon nanotubes for near-infrared light therapy of cancer

Whitney M Prickett[1,2]**, Brent D Van Rite**[1,2]**, Daniel E Resasco**[1] **and Roger G Harrison**[1,2]

[1] School of Chemical, Biological and Materials Engineering, University of Oklahoma,
100 East Boyd, Room T-335, Norman, OK 73019, USA
[2] Bioengineering Center, University of Oklahoma, 100 East Boyd, Room T-335, Norman,
OK 73019, USA

E-mail: rharrison@ou.edu

Abstract
A new approach for targeting carbon nanotubes to the tumor vasculature was tested using human endothelial cells and MCF-7 breast cancer cells *in vitro*. Single-walled carbon nanotubes were functionalized with the F3 peptide using a polyethylene glycol linker to target nucleolin, a protein found on the surface of endothelial cells in the vasculature of solid tumors. Confocal microscopy and Raman analysis confirmed that the conjugate was internalized by actively dividing endothelial cells. Dividing endothelial cells were used to mimic these cells in the tumor vasculature. Incubation with the conjugate for 8 h or more caused significant cell death in both actively dividing endothelial cells and MCF-7 breast cancer cells, an effect that is hypothesized to be due to the massive uptake of the conjugate. This targeted cell killing was further enhanced when coupled with near-infrared laser treatment. For confluent (non-dividing) endothelial cells, no cytotoxic effect was seen for incubation alone or incubation coupled with laser treatment. These results are promising and warrant further studies using this conjugate for cancer treatment *in vivo*.

(Some figures in this article are in colour only in the electronic version)

1. Introduction

Tumor growth depends on the ability of the tumor to form new blood vessels. It has been shown that cells cannot grow past the oxygen diffusion limit of about 150 μm [1]. So, tumor growth beyond 150 μm is dependent on angiogenesis, the sprouting of new blood vessels from existing ones [2]. Thus, targeting angiogenic blood vessels is a potential way to selectively treat cancerous tumors in the body.

The purpose of this research is to develop a treatment that is able to selectively target the vasculature of solid tumors and induce tumor cell death without harming the surrounding normal tissue. This study specifically focuses on the use of functionalized carbon nanotubes targeted to the tumor vasculature combined with near-infrared light therapy for breast cancer treatment.

Perhaps the most researched property of carbon nanotubes for cancer therapy in recent years has been their strong absorbance in the near-infrared light range (700–1400 nm). This property makes carbon nanotubes an enticing vehicle for selective cell killing because many biological tissues are transparent in the near-infrared range [3–5]. It is well documented that carbon nanotubes themselves are not toxic to cells but, when combined with near-infrared light therapy, they have been shown to cause cell death by thermal ablation [3, 6–10]. Nanotubes targeted to the tumor vasculature coupled with near-infrared light therapy will cause tumor endothelial cells in close proximity to die from the heat released and by cutting off the blood supply to the tumor.

Because they are actively dividing, tumor endothelial cells express specific markers that are not present on the surface of normal endothelial cells. One such cell

surface marker is nucleolin [11]. Nucleolin is a 105 kDa nucleolar phosphoprotein that is primarily found in the cell cytoplasm [12]. It has been shown to autocatalyze its own degradation; however, it is presumed that cell proliferation somehow inhibits this self-cleaving because intact nucleolin predominates in actively dividing cells, while non-dividing cells contain more degraded fragments of nucleolin [13]. It has also been shown that nucleolin is translocated to the cell surface during proliferation [14] and that proliferating cells express up to ten times as much nucleolin as cells in the stationary growth phase [12].

Endothelial cells within angiogenic blood vessels will be actively dividing and nucleolin has been confirmed to be present on the surface of these cells when they are dividing [15, 16]. One *in vivo* study using antinucleolin antibodies injected into mice bearing MDA-MB-435 tumors found that nucleolin was expressed on the surface of the angiogenic tumor blood vessels but was absent from the blood vessels of normal tissues [16]. Another study showed that the amount of nucleolin expressed on the surface of seven different cancer cell lines increased with decreasing doubling time [15]. The increased expression of nucleolin in proliferating endothelial and tumor cells makes it a potential target for homing to tumor vasculature.

The targeting moiety used in this study is the F3 peptide, a fragment of the high mobility group protein 2 [17]. F3 is a 31-amino-acid peptide that has been shown to home to the nuclei of tumor endothelial cells and tumor cells [17, 18] and bind to cell surface nucleolin and become internalized [16]. The use of F3 to target the tumor vasculature has been widely researched in recent years [17–19]. Human MDA-MB-435 breast cancer cells were found to internalize fluorescein-labeled F3 and translocate it to the cell nucleus *in vitro* and *in vivo* [17]. Another study in which F3 was linked to an α-particle-emitting isotope yielded similar results [19]. Two hundred times more of the F3 conjugate was found in the nucleus of cells tested *in vitro* than in the cellular supernatant and an *in vivo* test in mice-bearing tumors gave an increased survival when the F3 conjugate was injected, with no toxicity due to the treatment.

This study is the first to investigate targeting carbon nanotubes that have been functionalized with the F3 peptide. Single-walled carbon nanotubes (SWNTs) having a strong optical absorbance in the near-infrared range are used in order to have maximal heating of cells using photodynamic therapy. Following incubation with the SWNT–F3 conjugate, cells are irradiated with a near-infrared laser, and the cytotoxic effect is evaluated.

2. Methods

2.1. Preparation of SWNT–F3 conjugate

Single-walled carbon nanotubes (SG 65) were obtained from SouthWest NanoTechnologies (Norman, OK). The nanotubes are produced by the CoMoCAT® method and have a tube diameter of 0.8 nm. The majority of the nanotubes are (6, 5) chirality. A 1,2-distearoyl-*sn*-glycero-3-phosphoethanolamine-polyethylene glycol-maleimide (DSPE-PEG-maleimide) linker was purchased from Creative

PEGWorks (Winston Salem, NC). The F3 peptide (KDE-PQRRSARLSAKPAPPKPEPKPKKAPAKK) was synthesized with fluorescein isothiocyanate (FITC) added at the N-terminus and an extra cysteine residue at the C-terminus (Biomatik, Wilmington, DE).

SWNTs were suspended in 1% SDS (3 mg in 5 ml) through two cycles consisting of sonication at 7 W for 30 min followed by 30 min of centrifugation at $15\,680g$. The DSPE-PEG-maleimide linker was allowed to reach room temperature and was dissolved in 5 ml of deionized water (1 mg ml^{-1}). One milligram of the F3 peptide was reconstituted in 3 ml of PBS, pH 7.4 and allowed to mix with 1 ml of the linker solution at room temperature for 15 h. Unreacted ligand was blocked with L-cysteine for 1 h at a molar ratio of L-Cys/F3 of 7. An 8 h dialysis was performed using PBS at pH 7.4 with a buffer volume of 1 l and a membrane size of 2 kDa. The 4 ml F3-linker solution was then added to the 5 ml SWNT suspension and allowed to mix at room temperature for 30 min. A second 8 h dialysis was performed using deionized water with a buffer volume of 2 l and a membrane size of 100 kDa. The SWNT–F3 conjugate solution was then centrifuged at $15\,680g$ for 1 h to remove any existing SWNT aggregates. The F3 concentration was determined using the Bradford assay, and SWNT concentration was determined by measuring absorbance at 800 nm on a UV-2450 Shimadzu spectrophotometer and comparing to a standard curve.

2.2. Fluorescence and confocal microscopy

MCF-7 breast cancer cells were from the American Type Culture Collection (Manassas, VA), and HAAE-1 human aortic endothelial cells were from Coriell Cell Repositories (Camden, NJ). Cells were grown to 60–70% confluence on glass coverslips in 35 mm petri dishes overnight. The SWNT–F3 conjugate was diluted to 60 mg l^{-1} in cell medium (Eagle's minimum essential medium for MCF-7 cells and F12K medium for endothelial cells, both purchased from ATCC). The cell medium was removed from the petri dishes and 3 ml of the diluted conjugate was added to each petri dish. Cells were incubated with the conjugate for 2, 8, 16 or 24 h at 37 °C and 5% CO$_2$ then washed four times with medium. Prior to fluorescence microscopy (Nikon Eclipse E800 fluorescence microscope), a drop of Fluoro-gel with TES buffer (Fisher Scientific) was placed on a glass slide after the washing, and the coverglass was placed face-down on the gel drop to preserve fluorescence. Prior to confocal microscopy (Olympus Fluoview laser scanning microscope), the cells were stained with CellMask Deep Red plasma membrane stain (7.5 μg ml^{-1}; Invitrogen, Carlsbad, CA) for 30 min at 37 °C, washed, and fixed with 10% buffered formalin for 10 min at 37 °C. Fluoro-gel was added after the washing to preserve fluorescence.

2.3. Near-infrared laser testing

Endothelial cells and MCF-7 breast cancer cells were grown to 60–70% confluence in 24-well plates overnight. The SWNT–F3 conjugate was diluted to 60 mg l^{-1} in cell medium. The cell
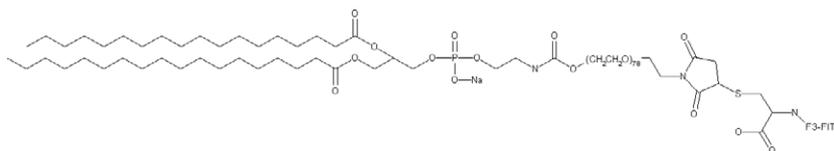
Figure 1. The F3 peptide was attached to a phospholipid–polyethylene-glycol linker via a reaction between a maleimide on the linker and an extra cysteine residue on the C-terminus of the peptide.

medium was removed from the plates and 300 μl of the diluted conjugate was added to each well. Cells were incubated with the conjugate for 2, 8, 16 or 24 h at 37 °C and 5% CO_2, washed four times with medium, and irradiated with an energy density of 350 J cm^{-2} at 980 nm (Diodevet-50 Laser, B&W TEK Inc., Newark, DE). Cells were incubated in their respective cell medium at 37 °C and 5% CO_2 for 1 h following laser treatment before measuring cell viability. The Alamar Blue assay was performed for measuring cell viability by adding Alamar Blue solution to each well to give 10% Alamar Blue and then incubated for 4 h at 37 °C. A portion of the solution (250 μl) was transferred to an opaque 96-well plate and the fluorescence was read at 590 nm with excitation at 530 nm using a microtiter plate reader. The blank consisted of wells containing only medium and Alamar Blue solution.

2.4. Raman spectra and analysis of SWNT–F3 conjugate

Samples for Raman analysis were prepared just as those for fluorescent microscopy. Raman spectra were taken using a Jovin Yvon-Horiba Lab spectrometer equipped with a CCD detector and with a laser excitation of 633 nm (He–Ne laser). Absorbance versus wavelength data was obtained using a spectrophotometer at SouthWest NanoTechnologies.

2.5. Data analysis

To test differences in cell viability, a one-way ANOVA employing a Tukey–Kramer multiple comparison test was performed using GraphPad InStat software (GraphPad; La Jolla, CA) with various significance (p) levels.

3. Results and discussion

3.1. SWNT–F3 conjugate preparation and near-infrared spectra

A polyethylene glycol linker containing a maleimide at one end and a phospholipid at the other is used to conjugate the F3 peptide to single-walled carbon nanotubes (SWNTs) (figure 1). The phospholipid portion of the linker is then conjugated to the SWNT through hydrophobic interaction with the SWNT surface. This construct was designed for targeting the SWNTs to the nucleolin receptor expressed on the surface of endothelial cells lining the tumor vasculature.

The absorbance characteristics of the conjugate solution were compared to that of SWNTs suspended in 1% SDS to determine if the conjugation process significantly changed the absorbance qualities of the nanotubes. Figure 2 shows a comparison of the normalized absorbance at varied
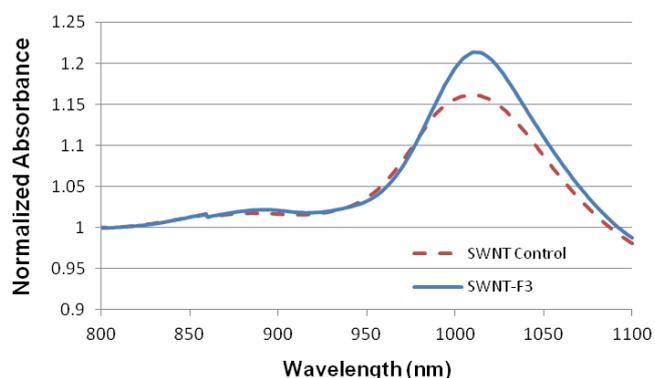

Figure 2. Comparison of the absorbance characteristic of SWNTs suspended in 1% SDS (SWNT control) and the SWNT–F3 conjugate.

wavelengths for both the SWNTs in 1% SDS (SWNT control) and the conjugate solution (SWNT–F3). A strong absorbance peak was still present after conjugation with no change in the wavelength at the maximum absorbance. The (6, 5) chirality SWNTs used have been shown to have a strong absorbance band at 980 nm [20]. However, absorbance peaks can be shifted depending on the species adsorbed [21, 22]. This is likely the cause of the shift to the right of 980 nm seen in figure 2. It is hypothesized that both the SDS and the F3-linker adsorbed to the nanotube surface caused a shift in the absorbance peak.

3.2. Binding and internalization of the SWNT–F3 conjugate

The binding ability of the conjugate was evaluated for both dividing endothelial cells and MCF-7 breast cancer cells. Cells were grown in petri dishes and incubated with the SWNT–F3 conjugate for 2, 8, 16 or 24 h. Binding of the conjugate was evaluated by fluorescent microscopy. Figure 3 shows fluorescent images for 2 and 16 h incubation times. Cells incubated for 2 and 8 h showed similar fluorescence intensity. Cells incubated for 16 h showed a significant increase in fluorescence intensity, indicating that more of the conjugate was binding. The intensity difference between 16 and 24 h of incubation was negligible (data not shown). Similar results were obtained for MCF-7 cancer cells. In the absence of the SWNT–F3 conjugate, there was no autofluorescence of either dividing endothelial cells or MCF-7 cancer cells.

Internalization of the conjugate was verified by confocal microscopy (figure 4) and Raman analysis (figure 5) for dividing endothelial cells. Using a confocal microscope, it was verified that the observed fluorescence was coming from
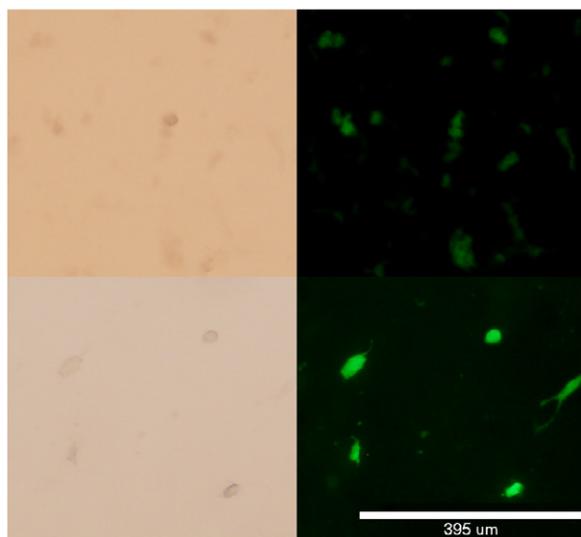
Figure 3. Dividing endothelial cells were incubated with the SWNT–F3 conjugate for up to 24 h and visualized under a fluorescence microscope. Images on the left are the bright-field images that correspond to the fluorescent images on the right. Cells incubated for 16 h (bottom) showed significantly more fluorescence than those incubated for only 2 h (top).
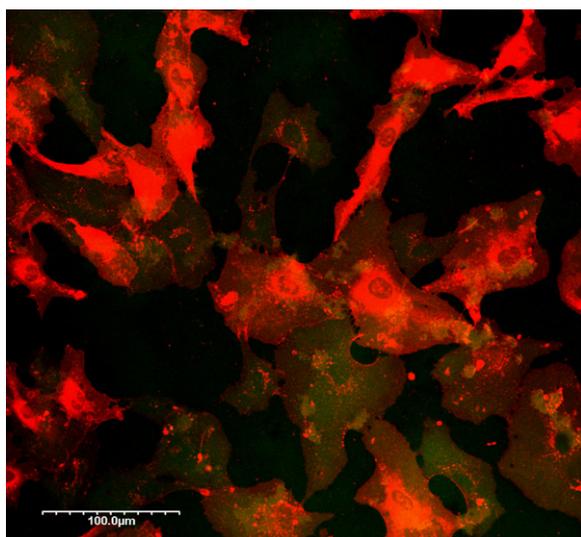

Figure 4. Confocal image of dividing endothelial cells following 12 h of incubation with the SWNT–F3 conjugate. Cellular membranes are stained in red with CellMask Deep Red. The green fluorescence is from the SWNT–F3 conjugate (F3 tagged at the N-terminus with FITC).

the inside of the cell, not just the surface (figure 4). The CellMask Deep Red stain delineated the cell membranes; green fluorescence from the SWNT–F3 conjugate was present in a substantial portion of the cell interiors. To confirm that this fluorescence indicated the presence of the SWNT–F3 conjugate and not F3 alone, the Raman spectra of a fluorescing cell was taken. Figure 5 shows the Raman spectra of a fluorescent endothelial cell after incubation with the SWNT–F3 conjugate for 16 h. The characteristic peak at 1590 cm^{-1} indicates the presence of SWNTs in the fluorescing cell. When the Raman
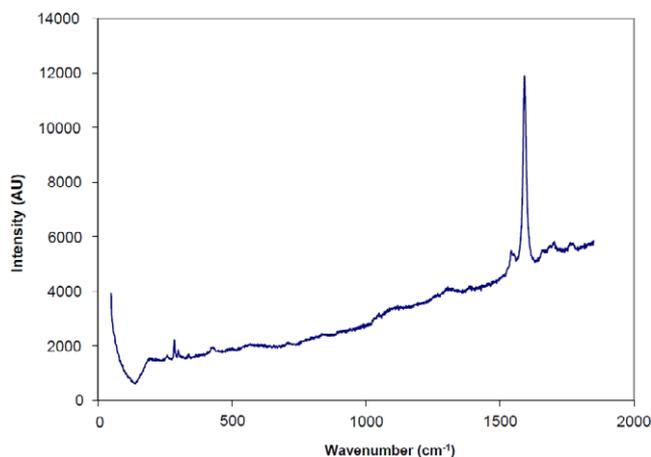
Figure 5. Raman spectra of a fluorescing endothelial cell following 16 h of incubation with the SWNT–F3 conjugate. The characteristic peak at 1590 cm^{-1} indicates the presence of SWNTs within the cell, confirming the internalization of the conjugate.
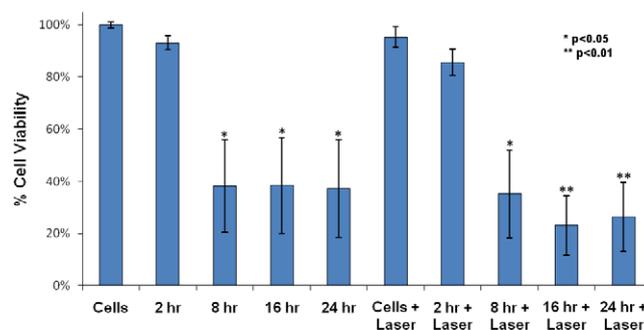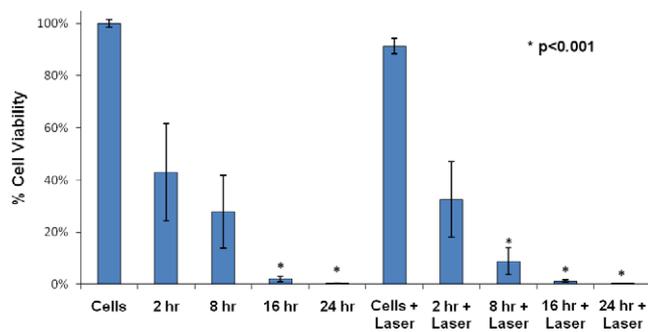

Figure 6. Effect on cell viability of incubation of dividing endothelial cells with the SWNT–F3 conjugate for various times either without laser treatment (left side) or with laser treatment (right side). Cell viability was evaluated by the Alamar Blue assay after each incubation time. Data are presented as $\pm$SE ($n = 9$) and statistical significance compared to untreated cells is denoted by * ($p < 0.05$) or ** ($p < 0.01$).

beam was not directed at cells, no peak at 1590 cm^{-1} was observed (data not shown).

3.3. In vitro killing of dividing endothelial cells and cancer cells

Dividing endothelial cells and MCF-7 cancer cells were grown in 24-well plates. Cells were incubated with 60 mg l^{-1} of the SWNT–F3 conjugate for up to 24 h, thoroughly washed and subjected to laser treatment at an energy density of 350 J cm^{-2}. One hour after laser treatment, cell viability was determined using the Alamar Blue assay (figures 6 and 7). Incubation with the conjugate alone caused significant cell death for both dividing endothelial cells and MCF-7 cells. Compared to untreated cells, the cell viability of endothelial cells after 24 h of incubation with the conjugate was reduced by 63% for the conjugate alone ($p < 0.05$) and by 74% for the conjugate with laser treatment ($p < 0.01$). For MCF-7 cells, the reductions in cell viability at 24 h compared to untreated cells were 99.7%

Figure 7. Effect on cell viability of incubation of MCF-7 cancer cells with the SWNT–F3 conjugate for various times either without laser treatment (left side) or with laser treatment (right side). Cell viability was evaluated by the Alamar Blue assay after each incubation time. Data are presented as $\pm$ SE ($n = 9$) and statistical significance compared to untreated cells is denoted by * ($p < 0.001$).
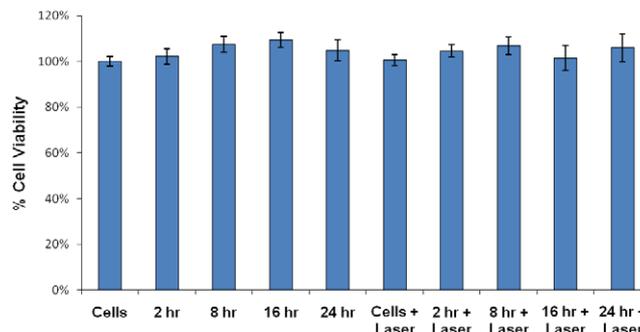
Figure 8. Effect on cell viability of incubation of confluent endothelial cells with the SWNT–F3 conjugate for various times either without laser treatment (left side) or with laser treatment (right side). Cell viability was evaluated by the Alamar Blue assay after each incubation time. Data are presented as $\pm$SE ($n = 9$). No groups were statistically different from untreated cells at $p < 0.05$.

for the conjugate alone and 99.8% for the conjugate with laser treatment ($p < 0.001$). Thus, the cell killing obtained by incubation with the conjugate was further enhanced with laser treatment, although this enhancement was not great. It is hypothesized that massive uptake of the SWNT–F3 conjugate into the dividing endothelial cells and MCF-7 cells caused cell lysis, which could explain the large amount of cell death from incubation with the conjugate alone. The greater cell killing of the MCF-7 cancer cells compared to the endothelial cells is probably because a fraction of the endothelial cells were in contact with other cells on all sides and were in a sense locally confluent, so that these cells did not express nucleolin on the cell surface and therefore would not bind to F3. On the other hand, F3 has been found to bind uniformly to cancer cells in tumor masses *in vivo* [17] and thus in our study we would expect all of the MCF-7 cells to bind to F3.

It is very likely that greater cell killing by the laser would have occurred had a *Q*-switched laser been used instead of a diode laser. In a study by Kang *et al* [23] of *Q*-switched laser treatment of cancer cells with SWNTs internalized, the significant killing of the cells obtained is believed to be due to a large photoacoustic effect, where a firecracker-like explosion is created by the *Q*-switched laser.

Another research group has attached the F3 peptide to polyacrylamide nanoparticles encapsulated with Photofrin, which is a photosensitizer [24]. An *in vitro* study in which MDA-MB-435 breast cancer cells were incubated with the conjugate and later subjected to laser irradiation resulted in 90% cell killing; however, non-targeted nanoparticles with laser irradiation of F3-nanoparticles without laser irradiation had no effect on cell viability. The mechanism of killing is by the light-activated photosensitizer interacting with molecular oxygen to produce cytotoxic singlet oxygen that leads to apoptotic and necrotic responses within cancer cells, which is a different mechanism than the heat-induced killing used in the current study. When analyzed by fluorescence microscopy, it was found that the nanoparticles bound to the surface of the MDA-MB-435 cells and were also internalized by the cells. In a study by a different group, F3 was used to deliver quantum

dots (qdots) to tumor blood vessels [25]. The F3-PEG-qdots were intravenously injected into mice bearing MDA-MB-435 xenograft tumors and were found to home onto the tumor blood vessels and become internalized by the cells. There were no detectable qdots found in the other tissues tested and no side effects in the mice were reported.

3.4. Selectivity of SWNT–F3 conjugate

The selectivity of the SWNT–F3 conjugate for dividing cancer endothelial cells versus confluent endothelial cells was then evaluated. Endothelial cells were grown to a confluent monolayer of cells in order to mimic the endothelial cells in normal blood vessels. The confluent (non-dividing) endothelial cells were then subjected to the same binding and *in vitro* laser killing tests as the MCF-7 cells and dividing endothelial cells. No fluorescence was observed for cells incubated with the conjugate for any of the tested time lengths. Cells also remained viable after incubation with the conjugate for all time lengths and after laser treatment following incubation (figure 8). These results suggest that the conjugate will not bind to normal endothelial cells in the body, since nucleolin has been found in *in vivo* studies to be absent from the blood vessels of other tissues [16]. Therefore, the targeted therapy will only affect tumor cells and endothelial cells within angiogenic blood vessels, where nucleolin has been shown in *in vivo* studies to be present on the cell surface [16].

To verify that the decrease in cellular viability of the dividing endothelial cells and MCF-7 cells following incubation with the SWNT–F3 conjugate and without laser treatment was due to uptake of the SWNT conjugate, another experiment was done. A conjugate was made that lacked the F3 targeting moiety. This control conjugate was made following the same protocol as before without the addition of the F3 peptide. Dividing endothelial cells were then incubated with this conjugate for 0, 2, 8, 16 or 24 h and not treated with the laser. No cell death was observed from incubation with the conjugate that lacked the targeting moiety (figure 9). This result suggests that the cytotoxic effect is dependent on the
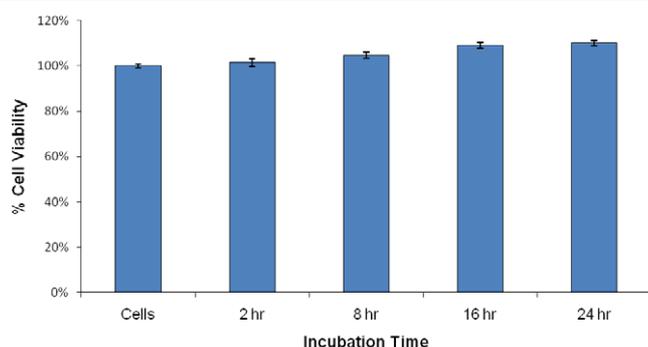
Figure 9. Effect on cell viability of incubation of confluent endothelial cells with the SWNT conjugate lacking F3 and not laser-treated. Cell viability was evaluated by the Alamar Blue assay after each incubation time. Data are presented as $\pm$SE ($n = 6$). No groups were statistically different from untreated cells at $p < 0.05$.

presence of the F3, supporting the idea that it is the uptake of the SWNT–F3 conjugate that causes a decrease in cellular viability in nucleolin expressing cells.

Possible toxicity of SWNTs administered systemically is a potential concern. However, in a biodistribution study by Liu *et al* [26], this was not found to be a problem; for mice injected i.v. with SWNT–PEG at a dosage up of 1 mg kg^{-1}, no obvious toxicity or negative health effects were observed over 3 months of monitoring. No mortality or significant loss of body weight was seen in any of the mice (>30). There was near-complete clearance of the SWNTs from the main organs in about 2 months. The biodistribution data suggested possible urinary and biliary excretion routes for the SWNTs.

4. Conclusion

This paper presents strong evidence that SWNTs conjugated to the F3 peptide have the ability to selectively target the nucleolin expressed in the tumor vasculature. Using confocal microscopy and Raman analysis, dividing endothelial cells, which are known to express nucleolin on their surface, were shown to internalize the SWNT–F3 conjugate. In contrast, confluent endothelial cells showed no binding of the conjugate by fluorescence microscopy. Significant cell death was observed in both dividing endothelial cells and MCF-7 cancer cells following incubation with the SWNT–F3 conjugate; while confluent endothelial cells, that do not express cell surface nucleolin, remained fully viable. The targeted cell killing of cells expressing surface nucleolin was further enhanced with near-infrared laser treatment. These *in vitro* results are promising and warrant further studies using this conjugate for cancer treatment *in vivo*.

Acknowledgments

References

[1] Goldacre R J and Sylven B 1962 On the access of blood-borne dyes to various tumor regions *Br. J. Cancer* **16** 306–22

[2] Hanahan D and Folkman J 1996 Patterns and emerging mechanisms of the angiogenic switch during tumorigenesis *Cell* **86** 353–64

[3] Kam N W S, O'Connell M, Wisdom J A and Dai H 2005 Carbon nanotubes as multifunctional biological transporters and near-infrared agents for selective cancer cell destruction *Proc. Natl Acad. Sci.* **102** 11600–5

[4] O'Neal D P, Hirsch L R, Halas N J, Payne J D and West J L 2004 Photo-thermal tumor ablation in mice using near infrared-absorbing nanoparticles *Cancer Lett.* **209** 171–6

[5] König K 2000 Multiphoton microscopy in life sciences *J. Microsc.* **200** 83–104

[6] Zhou F, Xing D, Ou Z, Wu B, Resasco D and Chen W 2009 Cancer photothermal therapy in the near-infrared region by using single-walled carbon nanotubes *J. Biomed. Opt.* **14** 021009

[7] Chakravarty P, Marches R, Zimmerman N S, Swafford A D-E, Bajaj P, Musselman I H, Pantano P, Draper R K and Vitetta E S 2008 Thermal ablation of tumor cells with antibody-functionalized single-walled carbon nanotubes *Proc. Natl. Acad. Sci.* **105** 8697–702

[8] Moon H K, Lee S H and Choi H C 2009 *In vivo* near-infrared mediated tumor destruction by photothermal effect of carbon nanotubes *ACS Nano* **3** 3707–13

[9] Shao N, Lu S, Wickstrom E and Panchapakesan B 2007 Integrated molecular targeting of IGF1R and HER2 surface receptors and destruction of breast cancer cells using single wall carbon nanotubes *Nanotechnology* **18** 315101

[10] Xiao Y *et al* 2009 Anti-HER2 IgY antibody-functionalized single-walled carbon nanotubes for detection and selective destruction of breast cancer cells *BMC Cancer* **9** 351

[11] Srivastava M and Pollard H B 1999 Molecular dissection of nucleolin's role in growth and cell proliferation: new insights *FASEB J.* **13** 1911–22

[12] Pfeifle J and Anderer F A 1983 Isolation and characterization of phosphoprotein pp 105 from Simian Virus 40-transformed mouse fibroblasts *Biochim. Biophys. Acta* **762** 86–93

[13] Chen C-M, Chiang S-Y and Yeh N-H 1991 Increased stability of nucleolin in proliferating cells by inhibition of its self-cleaving activity *J. Biol. Chem.* **266** 7754–8

[14] Hovanessian A G, Puvion-Dutilleul F, Nisole S, Svab J, Perret E, Deng J-S and Krust B 2000 The cell-surface-expressed nucleolin is associated with the actin cytoskeleton *Exp. Cell Res.* **261** 312–28

[15] Derenzini M, Sirri V, Trerè D and Ochs R 1995 The quantity of nucleolar proteins nucleolin and protein B23 is related to cell doubling time in human cancer cells *Lab. Invest.* **73** 497–502

[16] Christian S, Pilch J, Akerman M E, Porkka K, Laakkonen P and Ruoslahti E 2003 Nucleolin expressed at the cell surface is a marker of endothelial cells in angiogenic blood vessels *J. Cell Biol.* **163** 871–8

[17] Porkka K, Laakkonen P, Hoffman J A, Bernasconi M and Ruoslahti E 2002 A fragment of the HMGN2 protein homes to the nuclei of tumor cells and tumor endothelial cells *in vivo Proc. Natl. Acad. Sci.* **99** 7444–9

[18] Zhang Y, Yang M, Park J-H, Singelyn J, Ma H, Sailor M J, Ruoslahti E, Ozkan M and Ozkan C 2009 A surface-charge study on cellular-uptake behavior of F3-peptide-conjugated iron oxide nanoparticles *Small* **5** 1990–6

[19] Drecoll E *et al* 2009 Treatment of peritoneal carcinomatosis by targeted delivery of the radio-labeled tumor homing peptide ^{213}Bi-DTPA-[F3]$_2$ into the nucleus of tumor cells *PLoS One* **4** e5715

[20] Tan Y and Resasco D E 2005 Dispersion of single-walled carbon nanotubes of narrow diameter distribution *J. Phys. Chem.* **109** 14454–60

[21] Malik S, Vogel S, Rösner H, Arnold K, Hennrich F, Köhler A-K, Richert C and Kappes M M 2007 Physical chemical characterization of DNA–SWNT suspensions and associated composites *Compos. Sci. Technol.* **67** 916–21

[22] Palwai N R, Martyn D E, Neves L F F, Tan Y, Resasco D E and Harrison R G 2007 Retention of biological activity and near-infrared absorbance upon adsorption of horseradish peroxidase on single-walled carbon nanotubes *Nanotechnology* **18** 235601

[23] Kang B, Yu D, Dai Y, Chang S, Chen D and Ding Y 2009 Cancer-cell targeting and photoacoustic therapy using carbon nanotubes as 'bomb' agents *Small* **5** 1292–301

[24] Reddy G R *et al* 2006 Vascular targeted nanoparticles for imaging and treatment of brain tumors *Clin. Cancer Res.* **12** 6677–86

[25] Åkerman M E, Chan W C W, Laakkonen P, Bhatia S N and Ruoslahti E 2002 Nanocrystal targeting *in vivo Proc. Natl Acad. Sci.* **99** 12617–21

[26] Liu Z, Davis C, Cai W, He L, Chen X and Dai H 2008 Circulation and long-term fate of functionalized, biocompatible single-walled carbon nanotubes in mice probed by Raman Spectroscopy *Proc. Natl Acad. Sci.* **105** 1410–5